PERGAMON

International Journal of Solids and Structures 36 (1999) 2507–2525

INTERNATIONAL JOURNAL OF SOLIDS and STRUCTURES

A domain decomposition method for bodies with heterogeneous microstructure based on material regularization

T. Zohdi*, P. Wriggers

Institut für Mechanik, D-64289 Darmstadt, Germany

Received 29 March 1997; in revised form 12 March 1998

Abstract

A domain decomposition method is developed to reduce the computational complexity of boundary value problems associated with the structural analysis of bodies with arbitrary external geometry, loading and linearly elastic microstructure. The purpose of the method is to augment existing numerical discretization methods of analysis, such as the finite element method. The approach is to partition and decouple the heterogeneous body into more computationally tractable, nonoverlapping, subdomains whose union forms the entire domain under analysis. This is achieved by approximating the subdomain boundary conditions. The approximate boundary conditions, of displacement or traction type, are supplied from the solution to a relatively computationally inexpensive auxiliary boundary value problem characterized by a simple regularized microstructure. Since the decoupled subdomains may then be analyzed separately, the memory requirements are reduced and computing procedures are trivially parallelizable. A-posteriori error bounds are developed for solutions generated by this process. It is shown that, in the special case of uniform exterior loading, the error bounds collapse into forms which imply results pertaining to effective property ordering coinciding with those published by Huet (1990).

1. Introduction

In many modern scientific applications, microstructural fields within a macroscopic body are desired which require some sort of numerical simulation for their determination. However, in many cases, due to complex microstructure, highly oscillatory irregular micro-fields arise. For sufficient accuracy in such situations, standard methods, such as the finite element, require extremely fine numerical discretization meshes. Associated computational difficulties result primarily from two facts, (1) the memory of most computing machines in existence are incapable of storing the huge algebraic systems of equations associated with the numerical discretization of such problems and (2) even if the memory were available, the resulting algebraic systems are so

* Corresponding author. Fax: 00 49 6151 166869; E-mail: zohdi@sibelius.mechanik.th-darmstadt.de

0020–7683/99/$ - see front matter
PII: S0020–7683(98)00124–3

immense that they can require possibly weeks, months or years to solve, even with state of the art techniques.

In order to reduce the computational complexity associated with such micromechanical simulations, we introduce a domain decomposition strategy. The purpose of the method is to augment existing numerical discretization methods of analysis, such as the finite element method. The approach is to partition and decouple the heterogeneous structure into smaller, more computationally tractable, subdomains. Essentially this is achieved by approximating the boundary conditions on each interior subdomain interface belonging to the partition. Since the decoupled subdomains may then be analyzed separately, the memory and computing requirements are reduced, and can be solved trivially in parallel.

To perform the decomposition, three sets of boundary value problems are employed (Fig. 1):

- The exact problem (P-I): This boundary value problem has no approximations of any kind. This problem is never solved, but is used as a reference solution to judge the quality of an approximate solution. In this work the exact problem is one describing the deformation of a body with arbitrary external geometry, general nonuniform loading and linearly elastic microstructure.
- The regularized (decoupling) problem (P-II): This relatively computationally inexpensive boundary value problem has the same external boundary values and geometry as the exact problem (P-I), but with a regularized, linear or nonlinear, constitutive relation between the stress and strain. This constitutive relation can be as simple as a spatially constant linear elastic law, i.e. one with no microstructure. The purpose of this problem is to generate approximate boundary conditions for the subdomains, in order to decouple them.
- The decoupled subdomain problems (P-III): These decoupled boundary value problems are defined over nonoverlapping subdomains whose union forms the entire domain under analysis. The subdomain boundary value problems have the exact linearly elastic microstructure (same as P-I) but approximate displacement or traction boundary data supplied from the regularized solution (P-II). The total approximate microstructural solution is simply the assembly of the subdomain solutions, each restricted to its corresponding subdomain.

In general, the regularized solution and the subdomain solutions must be computed numerically. Therefore, when using the method, both a decoupling and a numerical error exist. The primary goal of this work is to determine the characteristics of the approximate microscopic fields produced by this process, and to bound the corresponding error in terms of computable quantities. The outline of the paper is as follows. In Section 2 the governing equations are laid down for construction of the approximate solutions. In Section 3 the properties of the approximate solution, primarily bounds on the error, are determined. In Section 4 the method is applied to the special case of determination of effective macroscopic properties of statistically representative volume elements. Finally, in Section 5, a summary is presented, along with some comments pertaining to extensions and future work.

2. Governing equations

We consider a structure composed of linearly elastic material which occupies an open bounded domain in $\Omega \in \mathbb{R}^3$. Its boundary is denoted $\partial\Omega$. The body is in static equilibrium under the action

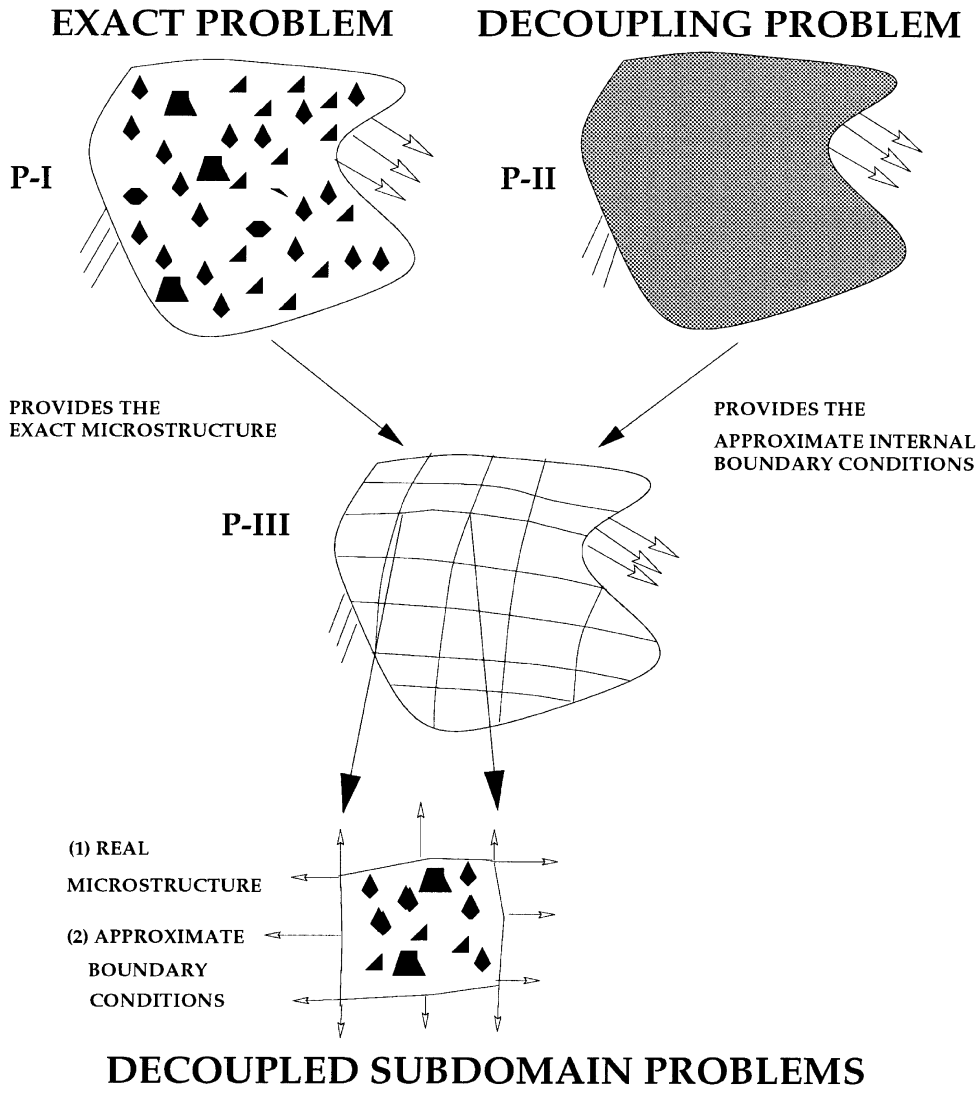

Fig. 1. Domain decomposition of a body with heterogeneous microstructure.

of body forces, $\boldsymbol{f}$, and surface tractions, $\boldsymbol{t}$. The boundary $\partial\Omega$ consists of a portion Γ_u on which the displacements, $\boldsymbol{d}$, are prescribed, and a part Γ_t on which tractions, $\boldsymbol{t}$, are prescribed. The microstructure is assumed to be perfectly bonded. We consider two possible decoupling approaches, (1) applied internal displacements and (2) applied internal tractions, separately.

2.1. The applied internal displacement approach

2.1.1. The exact problem formulation (*P-I*)

The exact solution, $\boldsymbol{u}$, is characterized by following the virtual work formulation of P-I:

$$\text{Find } \boldsymbol{u}, \boldsymbol{u}|_{\Gamma_u} = \boldsymbol{d}, \text{ such that} \int_\Omega \nabla \boldsymbol{v} : \boldsymbol{E} : \nabla \boldsymbol{u} \, \mathrm{d}\boldsymbol{x} = \int_\Omega \boldsymbol{f} \cdot \boldsymbol{v} \, \mathrm{d}\boldsymbol{x} + \int_{\Gamma_t} \boldsymbol{t} \cdot \boldsymbol{v} \, \mathrm{d}s \quad \forall \boldsymbol{v}, \boldsymbol{v}|_{\Gamma_u} = \boldsymbol{0}.$$

Here $\boldsymbol{E}$ is a fourth rank linear elasticity tensor with the usual symmetries and positive definite character. The components of $\boldsymbol{E}$ are functions of spatial position in the body.

2.1.2. The regularized decoupling problem formulation (P-II)

The regularized solution, $\boldsymbol{u}^R$, is characterized by a virtual work formulation of P-II:

$$\text{Find a } \boldsymbol{u}^R, \boldsymbol{u}^R|_{\Gamma_u} = \boldsymbol{d}, \text{ such that} \int_\Omega \nabla \boldsymbol{v} : \underbrace{\boldsymbol{R}(\nabla \boldsymbol{u}^R)}_{\boldsymbol{\sigma}^R} \mathrm{d}\boldsymbol{x} = \int_\Omega \boldsymbol{f} \cdot \boldsymbol{x} + \int_{\Gamma_t} \boldsymbol{t} \cdot \boldsymbol{v} \, \mathrm{d}s \quad \forall \boldsymbol{v}, \boldsymbol{v}|_{\Gamma_u} = \boldsymbol{0}.$$

Here the only requirement on $\boldsymbol{R}$ is that it produce an admissible $\boldsymbol{\sigma}^R$. $\boldsymbol{R}$ can be a linear or nonlinear constitutive response function. $\boldsymbol{R}$ can be as simple as a constant fourth-order linear elasticity tensor, and specific choices are given later in the paper.

2.1.3. Subdomain problems (P-III) and approximate solution construction

To construct the approximate microstructural solutions we first partition the domain, Ω, into N nonintersecting open subdomains $\overline{\cup_{K=1}^{N} \Omega_K} = \bar{\Omega}$. We define the boundary of an individual subdomain Ω_K, as $\partial\Omega_K$. When employing the applied internal displacement approach, the displacement solution to the virtual work formulation of the regularized problem (P-II) is projected onto the internal boundaries of the subdomain partitions. Any subdomain boundaries coinciding with the exterior surface retain their original boundary conditions. Accordingly, we have the following virtual work formulation, for each subdomain, $1 \leqslant K \leqslant N$:

$$\text{Find } \tilde{\boldsymbol{u}}_K^{R,ID}, \tilde{\boldsymbol{u}}_K^{R,ID}|_{\partial\Omega_K \cap (\Omega \cup \Gamma_u)} = \boldsymbol{u}^R, \text{ such that}$$

$$\int_{\Omega_K} \nabla \boldsymbol{v}_K : \boldsymbol{E} : \nabla \tilde{\boldsymbol{u}}_K^{R,ID} \, \mathrm{d}\boldsymbol{x} = \int_{\Omega_K} \boldsymbol{f} \cdot \boldsymbol{v}_K \, \mathrm{d}\boldsymbol{x} + \int_{\partial\Omega_K \cap \Gamma_t} \boldsymbol{t} \cdot \boldsymbol{v}_K \, \mathrm{d}s \quad \forall \boldsymbol{v}_K, \boldsymbol{v}_K|_{\partial\Omega_K \cap (\Omega \cup \Gamma_u)} = \boldsymbol{0}.$$

In this case the approximate solution is constructed by a direct assembly process

$$\underbrace{\tilde{\boldsymbol{u}}^{R,ID}}_{\text{approx. sol.}} \overset{\text{def}}{=} \underbrace{\boldsymbol{u}^R}_{\text{reg. sol.}} + \underbrace{(\tilde{\boldsymbol{u}}_1^{R,ID} - \boldsymbol{u}^R)|_{\Omega_1}}_{\text{subd. perturbation}} + \cdots + \underbrace{(\tilde{\boldsymbol{u}}_N^{R,ID} - \boldsymbol{u}^R)|_{\Omega_N}}_{\text{subd. perturbation}},$$

where the above parenthetical terms can be viewed as subdomain perturbations to the relatively smooth solution, $\boldsymbol{u}^R$.

2.2. The applied internal traction approach

We now outline the applied internal traction approach. Here complementary variational principles are used. The complementary variational principle for the exact problem (P-I) for the applied internal traction case is:

Find $\boldsymbol{\sigma}$, $\nabla\cdot\boldsymbol{\sigma}+\boldsymbol{f}=\boldsymbol{0}$, $\boldsymbol{\sigma}\cdot\boldsymbol{n}|_{\Gamma_t}=\boldsymbol{t}$, such that

$$\int_{\Omega}\boldsymbol{\tau}:\boldsymbol{E}^{-1}:\boldsymbol{\sigma}\,\mathrm{d}\boldsymbol{x}=\int_{\Gamma_u}\boldsymbol{\tau}\cdot\boldsymbol{n}\cdot\boldsymbol{d}\,\mathrm{d}s\quad\forall\boldsymbol{\tau},\nabla\cdot\boldsymbol{\tau}=\boldsymbol{0},\boldsymbol{\tau}\cdot\boldsymbol{n}|_{\Gamma_t}=\boldsymbol{0}.$$

The complementary variational formulation for the regularized decoupling problem is:

Find a $\boldsymbol{\sigma}^L$, $\nabla\cdot\boldsymbol{\sigma}^L+\boldsymbol{f}=\boldsymbol{0}$, $\boldsymbol{\sigma}^L\cdot\boldsymbol{n}|_{\Gamma_t}=\boldsymbol{t}$, such that

$$\int_{\Omega}\boldsymbol{\tau}:\underbrace{\boldsymbol{L}(\boldsymbol{\sigma}^{-1})}_{\boldsymbol{\varepsilon}^L}\,\mathrm{d}\boldsymbol{x}=\int_{\Gamma_u}\boldsymbol{\tau}\cdot\boldsymbol{n}\cdot\boldsymbol{d}\,\mathrm{d}s\quad\forall\boldsymbol{\tau},\nabla\cdot\boldsymbol{\tau}=\boldsymbol{0},\boldsymbol{\tau}\cdot\boldsymbol{n}|_{\Gamma_t}=\boldsymbol{0}.$$

As with $\boldsymbol{R}$, $\boldsymbol{L}$ can be linear or nonlinear, provided it produces an admissible $\boldsymbol{\varepsilon}^L$. In the case when $\boldsymbol{R}$ and $\boldsymbol{L}$ are linear elasticity tensors, then $\boldsymbol{L}=\boldsymbol{R}^{-1}$. For the general nonlinear case, if $\boldsymbol{R}$ has a unique inverse, then it is $\boldsymbol{L}$, and $\boldsymbol{u}^R=\boldsymbol{u}^L$ and $\boldsymbol{\sigma}^R=\boldsymbol{\sigma}^L$.

The complementary variational formulation for the applied internal traction case, consists of projecting tractions, constructed from the solution to complementary formulation of the regularized problem (P-II), onto the internal boundaries of the sub-domain partitions. Accordingly, we have the following complementary virtual work formulation, for each subdomain $1\leqslant K\leqslant N$:

Find $\tilde{\boldsymbol{\sigma}}_K^{L,IS}$, $\nabla\cdot\tilde{\boldsymbol{\sigma}}_K^{L,IS}+\boldsymbol{f}=\boldsymbol{0}$, $\boldsymbol{\sigma}^{L,IS}\cdot\boldsymbol{n}|_{\Gamma_t}=\boldsymbol{t}$, such that

$$\int_{\Omega_K}\boldsymbol{\tau}_K:\boldsymbol{E}^{-1}:\tilde{\boldsymbol{\sigma}}_K^{L,IS}\,\mathrm{d}\boldsymbol{x}=\int_{\partial\Omega_K\cap\nabla_{K_u}}\boldsymbol{\tau}_K\cdot\boldsymbol{n}_K\cdot\boldsymbol{d}\,\mathrm{d}s\quad\forall\boldsymbol{\tau}_K,\nabla\cdot\boldsymbol{\tau}_K=\boldsymbol{0},\boldsymbol{\tau}_K\cdot\boldsymbol{n}|_{\partial\Omega_K\cap(\Omega\cup\Gamma_t)}=\boldsymbol{0}.$$

The final stress field is constructed in the following manner

$$\underbrace{\tilde{\boldsymbol{\sigma}}^{L,IS}}_{\text{approx. sol.}}\overset{\text{def}}{=}\underbrace{\boldsymbol{\sigma}^L}_{\text{reg. sol.}}+\underbrace{(\tilde{\boldsymbol{\sigma}}_1^{L,IS}-\boldsymbol{\sigma}^L)|_{\Omega_1}}_{\text{subd. perturbation}}+\cdots+\underbrace{(\tilde{\boldsymbol{\sigma}}_N^{L,IS}-\boldsymbol{\sigma}^L)|_{\Omega_N}}_{\text{subd. perturbation}}.$$

3. Approximate solution properties

3.1. Characterization of the error

Since we employ energy-type variational principles to generate approximate solutions, we use the following associated energy norms to measure the error between solutions,

$$\|\boldsymbol{u}-\boldsymbol{w}\|_{E(\Omega)}^2\overset{\text{def}}{=}\int_{\Omega}\nabla(\boldsymbol{u}-\boldsymbol{w}):\boldsymbol{E}:\nabla(\boldsymbol{u}-\boldsymbol{w})\,\mathrm{d}\boldsymbol{x},\quad\|\boldsymbol{\sigma}-\boldsymbol{\gamma}\|_{E^{-1}(\Omega)}^2\overset{\text{def}}{=}\int_{\Omega}(\boldsymbol{\sigma}-\boldsymbol{\gamma}):\boldsymbol{E}^{-1}:(\boldsymbol{\sigma}-\boldsymbol{\gamma})\,\mathrm{d}\boldsymbol{x},$$

where $\boldsymbol{w}$ and $\boldsymbol{\gamma}$ are arbitrary admissible functions. Integration by parts yields (with $\boldsymbol{w}=\tilde{\boldsymbol{u}}^{R,ID}$ and $\boldsymbol{\gamma}=\tilde{\boldsymbol{\sigma}}^{L,IS}$)

$$\|\boldsymbol{u}-\tilde{\boldsymbol{u}}^{R,ID}\|_{E(\Omega)}^2=\sum_{K=1}^{N}\int_{\partial\Omega_K\cap\Omega}\underbrace{(\boldsymbol{E}:\nabla\tilde{\boldsymbol{u}}_K^{R,ID})\cdot\boldsymbol{n}_K}_{\text{not continuous at interface}}\cdot\underbrace{(\boldsymbol{u}_K^R-\boldsymbol{u})}_{\text{error in displacements}}\,\mathrm{d}s,$$

$$\|\boldsymbol{u}-\tilde{\boldsymbol{u}}^{R,ID}\|^2_{E(\Omega)} = \sum_{\mathscr{I}=1}^{N_{\mathscr{I}}} \int_{\Gamma_{\mathscr{I}}} (\text{traction jump}) \cdot (\text{error in displacements}) \, \mathrm{d}\boldsymbol{s},$$

$$\|\boldsymbol{\sigma}-\tilde{\boldsymbol{\sigma}}^{L,IS}\|^2_{E^{-1}(\Omega)} = \sum_{K=1}^{N} \int_{\partial\Omega_K\cap\Omega} \underbrace{(\boldsymbol{\sigma}_K^L-\boldsymbol{\sigma})\cdot\boldsymbol{n}_K}_{\text{error in tractions}} \cdot \underbrace{\tilde{\boldsymbol{u}}_K^{L,IS}}_{\text{not continuous at interface}} \, \mathrm{d}\boldsymbol{s},$$

$$\|\boldsymbol{\sigma}-\tilde{\boldsymbol{\sigma}}^{L,IS}\|^2_{E^{-1}(\Omega)} = \sum_{\mathscr{I}=1}^{N_{\mathscr{I}}} \int_{\Gamma_{\mathscr{I}}} (\text{error in tractions}) \cdot (\text{displacement jump}) \, \mathrm{d}\boldsymbol{s}, \tag{1}$$

where $\Gamma_{\mathscr{I}}$ is an interior subdomain interface, and $\mathscr{I} = 1, 2, \ldots, N_{\mathscr{I}}$ = number of interior subdomain interfaces. For the applied internal displacement case, the tractions may suffer discontinuities at the interior subdomain boundaries, while for the applied internal traction case, the displacements may be discontinuous at interior subdomain boundaries.

3.2. General error bounds

While the characterizations of the error in Equation set (1) provide some intuitive basis to characterize the nature of the error in the two decomposition approaches, they are essentially useless to judge the quality of the approximate solution, since they require knowledge of the exact solution. Therefore the goal is to bound the error in terms of known computed quantities, i.e. the computed subdomain solutions, and the regularized decoupling solution. In order to do this, we use the Principle of Minimum Potential Energy (PMPE) and the Principle of Minimum Complementary Potential Energy (PMCPE). We define the global elastic potentials as follows

$$\mathscr{J}(\boldsymbol{w}) \stackrel{\text{def}}{=} \frac{1}{2}\int_{\Omega} \nabla\boldsymbol{w} : \boldsymbol{E} : \nabla\boldsymbol{w} \, \mathrm{d}\boldsymbol{x} - \int_{\Omega} \boldsymbol{f}\cdot\boldsymbol{w} \, \mathrm{d}\boldsymbol{x} - \int_{\Gamma_t} \boldsymbol{t}\cdot\boldsymbol{w} \, \mathrm{d}s,$$

$$\mathscr{K}(\boldsymbol{\gamma}) \stackrel{\text{def}}{=} \frac{1}{2}\int_{\Omega} \boldsymbol{\gamma} : \boldsymbol{E}^{-1} : \boldsymbol{\gamma} \, \mathrm{d}\boldsymbol{x} - \int_{\Gamma_u} \boldsymbol{\gamma}\cdot\boldsymbol{n}\cdot\boldsymbol{d} \, \mathrm{d}s,$$

and the corresponding elastic subdomain potentials

$$\mathscr{J}_K(\boldsymbol{w}) \stackrel{\text{def}}{=} \frac{1}{2}\int_{\Omega_K} \nabla\boldsymbol{w} : \boldsymbol{E} : \nabla\boldsymbol{w} \, \mathrm{d}\boldsymbol{x} - \int_{\Omega_K} \boldsymbol{f}\cdot\boldsymbol{w} \, \mathrm{d}\boldsymbol{x} - \int_{\partial\Omega_K\cap\Gamma_t} \boldsymbol{t}\cdot\boldsymbol{w} \, \mathrm{d}s,$$

$$\mathscr{K}_K(\boldsymbol{\gamma}) \stackrel{\text{def}}{=} \frac{1}{2}\int_{\Omega_K} \boldsymbol{\gamma} : \boldsymbol{E}^{-1} : \boldsymbol{\gamma} \, \mathrm{d}\boldsymbol{x} - \int_{\partial\Omega_K\cap\Gamma_u} \boldsymbol{\gamma}\cdot\boldsymbol{n}_K\cdot\boldsymbol{d} \, \mathrm{d}s.$$

Determination of the error in terms of known quantities is straightforward. We first consider the applied internal displacement approach. For any admissible $\boldsymbol{w}$, we have from the PMPE, $\|\boldsymbol{u}-\boldsymbol{w}\|^2_{E(\Omega)} = 2\mathscr{J}(\boldsymbol{w}) - 2\mathscr{J}(\boldsymbol{u})$. By applying the PMPE, with $\boldsymbol{w} = \boldsymbol{u}^R$, we obtain

$$\|\boldsymbol{u}-\boldsymbol{u}^R\|^2_{E(\Omega)} = 2(\mathscr{J}(\boldsymbol{u}^R) - \mathscr{J}(\boldsymbol{u})) \Rightarrow \mathscr{J}(\boldsymbol{u}) = \mathscr{J}(\boldsymbol{u}^R) - \tfrac{1}{2}\|\boldsymbol{u}-\boldsymbol{u}^R\|^2_{E(\Omega)}.$$

Again applying the PMPE, with $\boldsymbol{w} = \tilde{\boldsymbol{u}}^{R,ID}$, we obtain

$$\|\boldsymbol{u}-\tilde{\boldsymbol{u}}^{R,ID}\|^2_{E(\Omega)} = 2(\mathscr{J}(\tilde{\boldsymbol{u}}^{R,ID})-\mathscr{J}(\boldsymbol{u})) = 2(\mathscr{J}(\tilde{\boldsymbol{u}}^{R,ID})-\mathscr{J}(\boldsymbol{u}^R))+\|\boldsymbol{u}-\boldsymbol{u}^R\|^2_{E(\Omega)}.$$

Since $\tilde{\boldsymbol{u}}^{R,ID}_K$ is a solution to a subdomain boundary value problem posed over Ω_K, it minimizes the corresponding subdomain potential energy function $\mathscr{J}_K(\cdot)$. Therefore

$$\mathscr{J}(\boldsymbol{u}^R) = \sum_{K=1}^{N} \mathscr{J}_K(\boldsymbol{u}^R_K) \geqslant \sum_{K=1}^{N} \mathscr{J}_K(\tilde{\boldsymbol{u}}^{R,ID}_K) = \mathscr{J}(\tilde{\boldsymbol{u}}^{R,ID}).$$

Consequently,

$$\|\boldsymbol{u}-\tilde{\boldsymbol{u}}^{R,ID}\|^2_{E(\Omega)} = \underbrace{2(\mathscr{J}(\tilde{\boldsymbol{u}}^{R,ID})-\mathscr{J}(\boldsymbol{u}^R))}_{\text{negative}}+\|\boldsymbol{u}-\boldsymbol{u}^R\|E^2_{E(\Omega)}.$$

We must now bound $\|\mathbf{u}-\mathbf{u}^R\|_{E(\Omega)}$ to obtain error estimate solely in terms of computable quantities. By definition

$$\int_\Omega \nabla\boldsymbol{v}\colon\boldsymbol{E}\colon\nabla\boldsymbol{u}\,\mathrm{d}\boldsymbol{x} = \int_\Omega \nabla\boldsymbol{v}\colon\boldsymbol{R}(\nabla\boldsymbol{u}^R)\,\mathrm{d}\boldsymbol{x} = \int_\Omega \boldsymbol{f}\cdot\boldsymbol{v}\,\mathrm{d}\boldsymbol{x}+\int_{\Gamma_t}\boldsymbol{t}\cdot\boldsymbol{v}\,\mathrm{d}s,$$

and subtracting $\int_\Omega \nabla\boldsymbol{v}\colon\boldsymbol{E}\colon\nabla\boldsymbol{u}^R\,\mathrm{d}\boldsymbol{x}$ from both sides yields

$$\int_\Omega \nabla\boldsymbol{v}\colon\boldsymbol{E}\colon\nabla(\boldsymbol{u}-\boldsymbol{u}^R)\,\mathrm{d}\boldsymbol{x} = \int_\Omega \nabla\boldsymbol{v}\colon(\boldsymbol{R}(\nabla\boldsymbol{u}^R)-\boldsymbol{E}\colon\nabla\boldsymbol{u}^R)\,\mathrm{d}\boldsymbol{x}.$$

Since $\boldsymbol{v}$ is an arbitrary virtual displacement, we may set $\boldsymbol{v}=\boldsymbol{u}-\boldsymbol{u}^R$ to yield

$$\begin{aligned}
\|\boldsymbol{u}-\boldsymbol{u}^R\|^2_{E(\Omega)} &= \int_\Omega \nabla(\boldsymbol{u}-\boldsymbol{u}^R)\colon(\boldsymbol{R}(\nabla\boldsymbol{u}^R)-\boldsymbol{E}\colon\nabla\boldsymbol{u}^R)\,\mathrm{d}\boldsymbol{x}\\
&= \int_\Omega \boldsymbol{E}^{1/2}\colon\nabla(\boldsymbol{u}-\boldsymbol{u}^R)\colon\boldsymbol{E}^{1/2}\colon\boldsymbol{E}^{-1}\colon(\boldsymbol{R}(\nabla\boldsymbol{u}^R)-\boldsymbol{E}\colon\nabla\boldsymbol{u}^R)\,\mathrm{d}\boldsymbol{x}\\
&\leqslant \underbrace{\left\{\int_\Omega \nabla(\boldsymbol{u}-\boldsymbol{u}^R)\colon\boldsymbol{E}\colon\nabla(\boldsymbol{u}-\boldsymbol{u}^R)\,\mathrm{d}\boldsymbol{x}\right\}^{1/2}}_{\|\mathbf{u}-\mathbf{u}^R\|_{E(\Omega)}}\\
&\quad\times\left\{\int_\Omega (\boldsymbol{R}(\nabla\boldsymbol{u}^R)-\boldsymbol{E}\colon\nabla\boldsymbol{u}^R)\colon\boldsymbol{E}^{-1}\colon(\boldsymbol{R}(\nabla\boldsymbol{u}^R)-\boldsymbol{E}\colon\nabla\boldsymbol{u}^R)\,\mathrm{d}\boldsymbol{x}\right\}^{1/2}.
\end{aligned}$$

Therefore,

$$\|\boldsymbol{u}-\boldsymbol{u}^R\|^2_{E(\Omega)} \leqslant \int_\Omega (\boldsymbol{E}\colon\nabla\boldsymbol{u}^R-\boldsymbol{R}(\nabla\boldsymbol{u}^R))\colon\boldsymbol{E}^{-1}\colon(\boldsymbol{E}\colon\nabla\boldsymbol{u}^R-\boldsymbol{R}(\nabla\boldsymbol{u}^R))\,\mathrm{d}\boldsymbol{x} \stackrel{\text{def}}{=} \zeta^2(\boldsymbol{u}^R). \tag{2}$$

Repeating the process for the applied internal traction case, using the PMCPE and the complementary variational formulations, we obtain

$$\|\boldsymbol{\sigma}-\tilde{\boldsymbol{\sigma}}^{L,IS}\|^2_{E^{-1}(\Omega)} = \underbrace{2(\mathscr{K}(\tilde{\boldsymbol{\sigma}}^{L,IS})-\mathscr{K}(\boldsymbol{\sigma}^L))}_{\text{negative}} + \|\boldsymbol{\sigma}-\boldsymbol{\sigma}^L\|^2_{E^{-1}(\Omega)},$$

$$\|\boldsymbol{\sigma}-\tilde{\boldsymbol{\sigma}}^{L,IS}\|_{E^{-1}(\Omega)} \leqslant \|\boldsymbol{\sigma}-\boldsymbol{\sigma}^L\|_{E^{-1}(\Omega)},$$

and

$$\|\boldsymbol{\sigma}-\boldsymbol{\sigma}^L\|^2_{E(\Omega)} \leqslant \int_\Omega (\boldsymbol{E}^{-1}:\boldsymbol{\sigma}^L-\boldsymbol{L}(\boldsymbol{\sigma}^L)):\boldsymbol{E}:(\boldsymbol{E}^{-1}:\boldsymbol{\sigma}^L-\boldsymbol{L}(\boldsymbol{\sigma}^L))\,\mathrm{d}\boldsymbol{x} \stackrel{\text{def}}{=} \beta^2(\boldsymbol{\sigma}^L). \tag{3}$$

In summary, for general loading and arbitrary microstructure, with an arbitrary linear or nonlinear decoupling material, we have the following decomposition error bounds,

$$\begin{aligned}
&0 \leqslant \|\boldsymbol{u}-\tilde{\boldsymbol{u}}^{R,ID}\|^2_{E(\Omega)} \leqslant \Psi^2(\tilde{\boldsymbol{u}}^{R,ID},\boldsymbol{u}^R,\zeta(\boldsymbol{u}^R)) \leqslant \zeta^2(\boldsymbol{u}^R),\\
&0 \leqslant \|\boldsymbol{\sigma}-\tilde{\boldsymbol{\sigma}}^{L,IS}\|^2_{E^{-1}(\Omega)} \leqslant \Phi^2(\tilde{\boldsymbol{\sigma}}^{L,IS},\boldsymbol{\sigma}^L,\beta(\boldsymbol{\sigma}^L)) \leqslant \beta^2(\boldsymbol{\sigma}^L),\\
&\Psi^2(\tilde{\boldsymbol{u}}^{R,ID},\boldsymbol{u}^R,\zeta(\boldsymbol{u}^R)) \stackrel{\text{def}}{=} 2(\mathscr{J}(\tilde{\boldsymbol{u}}^{R,ID})-\mathscr{J}(\boldsymbol{u}^R))+\zeta^2(\boldsymbol{u}^R),\\
&\Phi^2(\tilde{\boldsymbol{\sigma}}^{L,IS},\boldsymbol{\sigma}^L,\beta(\boldsymbol{\sigma}^L)) \stackrel{\text{def}}{=} 2(\mathscr{K}(\tilde{\boldsymbol{\sigma}}^{L,IS})-\mathscr{K}(\boldsymbol{\sigma}^L))+\beta^2(\boldsymbol{\sigma}^L).
\end{aligned} \tag{4}$$

Obviously these bounds require the computation of the decoupled subdomain solutions and the regularized decoupling solution. In general, the approximate solutions must be computed numerically. Therefore, the only available quantities to use in the error estimates in Equation set (4) are the discrete approximations to be regularized and subdomain solutions. The goal now is to determine the effect of the numerical discretization on the decomposition error bounds. We purposely leave the method of discretization for the variational formulations open.

3.3. Influence of numerical discretization

We first consider the applied internal displacement case. There are three sources of discretization error:

(1) Discretization error in the regularized decoupling problem: for the regularized decoupling problem we have

Find a $\boldsymbol{u}^{R,H}$, $\boldsymbol{u}^{R,H}|_{\Gamma_u} = \boldsymbol{d}$, such that

$$\underbrace{\int_\Omega \nabla \boldsymbol{v}^H:\boldsymbol{R}(\nabla \boldsymbol{u}^{R,H})\,\mathrm{d}\boldsymbol{x}}_{\mathscr{B}^R(\mathbf{u}^{R,H},\mathbf{v}^H)} = \underbrace{\int_\Omega \boldsymbol{f}\cdot\boldsymbol{v}^H\,\mathrm{d}\boldsymbol{x}+\int_{\Gamma_t}\boldsymbol{t}\cdot\boldsymbol{v}^H\,\mathrm{d}s}_{\mathscr{F}(\mathbf{v}^H)} \quad \forall \boldsymbol{v}^H,\ \boldsymbol{v}^H|_{\Gamma_u}=\mathbf{0}.$$

Here H signifies that some type of discretization has taken place for the regularized decoupling problem.

(2) Pure subdomain discretization error: for the subdomain problems, assuming no error in the regularized decoupling solution

Find $\tilde{\boldsymbol{u}}_K^{R,ID,h}$, $\tilde{\boldsymbol{u}}_K^{R,ID,h}|_{\partial\Omega_K\cap(\Omega\cup\Gamma_u)} = \boldsymbol{u}^R$, such that

$$\underbrace{\int_{\Omega_K} \nabla \boldsymbol{v}_K^h : \boldsymbol{E} : \nabla \tilde{\boldsymbol{u}}_K^{R,ID,h}\, \mathrm{d}\boldsymbol{x}}_{\mathscr{B}_K(\tilde{\boldsymbol{u}}_K^{R,ID,h},\, \boldsymbol{v}_K^h)} = \underbrace{\int_{\Omega_K} \boldsymbol{f}\cdot\boldsymbol{v}_K^h\, \mathrm{d}\boldsymbol{x} + \int_{\partial\Omega_K\cap\Gamma_t} \boldsymbol{t}\cdot\boldsymbol{v}_K^h\, \mathrm{d}s}_{\mathscr{F}(\boldsymbol{v}_K^h)} \quad \forall \boldsymbol{v}_K^h,\ \boldsymbol{v}_K^h|_{\partial\Omega_K\cap(\Omega\cup\Gamma_u)} = \boldsymbol{0},$$

$$\tilde{\boldsymbol{u}}^{R,ID,h} \overset{\text{def}}{=} \boldsymbol{u}^R + \sum_{K=1}^{N} (\tilde{\boldsymbol{u}}_K^{R,ID,h} - \boldsymbol{u}^R)|_{\Omega_K}.$$

Here h signifies that some type of discretization has taken place for the subdomain problems.

(3) Combined error: for the subdomain problems, assuming that there is discretization error in the regularized decoupling solution (which will pollute the imposed subdomain boundary conditions):

Find $\tilde{\boldsymbol{u}}_K^{R,ID,H,h}$, $\tilde{\boldsymbol{u}}_K^{R,ID,H,h}|_{\partial\Omega_K\cap(\Omega\Gamma_u)} = \boldsymbol{u}^{R,H}$, such that

$$\underbrace{\int_{\Omega_K} \nabla \boldsymbol{v}_K^{H,h} : \boldsymbol{E} : \nabla \tilde{\boldsymbol{u}}_K^{R,ID,H,h}\, \mathrm{d}\boldsymbol{x}}_{\mathscr{B}_K(\tilde{\mathbf{u}}_K^{R,ID,H,h},\, \mathbf{v}_K^{H,h})} = \underbrace{\int_{\Omega_K} \boldsymbol{f}\cdot\boldsymbol{v}_K^{H,h}\, \mathrm{d}\boldsymbol{x} + \int_{\partial\Omega_K\cap\Gamma_t} \boldsymbol{t}\cdot\boldsymbol{v}_K^{H,h}\, \mathrm{d}s}_{\mathscr{F}(\mathbf{v}_K^{H,h})} \quad \forall \boldsymbol{v}_K^{H,h},\ \boldsymbol{v}_K^{H,h}|_{\partial\Omega_K\cap(\Omega\cup\Gamma_u)} = \boldsymbol{0},$$

$$\tilde{\boldsymbol{u}}^{R,ID,H,h} \overset{\text{def}}{=} \boldsymbol{u}^{R,H} + \sum_{K=1}^{N} (\tilde{\boldsymbol{u}}_K^{R,ID,H,h} - \boldsymbol{u}^{R,H})|_{\Omega_K}.$$

Here the superscript, (H,h) signifies that the local subdomain problems have been discretized (h) and have received boundary data from the discretized regularized problem (H).

For brevity, let us define the following

(1) $\mathbf{e}^{R,H} \overset{\text{def}}{=} \boldsymbol{u}^{R,H} - \boldsymbol{u}^R$,

(2) $\mathbf{e}_K^h \overset{\text{def}}{=} \tilde{\boldsymbol{u}}_K^{R,ID,h} - \tilde{\boldsymbol{u}}_K^{R,ID}$ and $\mathbf{e}^h \overset{\text{def}}{=} \tilde{\boldsymbol{u}}^{R,ID,h} - \tilde{\boldsymbol{u}}^{R,ID}$,

(3) $\mathbf{e}_K^{H-h} \overset{\text{def}}{=} \tilde{\boldsymbol{u}}_K^{R,ID,H,h} - \tilde{\boldsymbol{u}}_K^{R,ID,h}$ and $\mathbf{e}^{H-h} \overset{\text{def}}{=} \tilde{\boldsymbol{u}}^{R,ID,H,h} - \tilde{\boldsymbol{u}}^{R,ID,h}$,

(4) $$\Lambda(\boldsymbol{u}^R, \boldsymbol{u}^{R,H}) \overset{\text{def}}{=} \zeta^2(\boldsymbol{u}^{R,H}) - \zeta^2(\boldsymbol{u}^R) = \underbrace{\int_{\Omega} (\boldsymbol{E}:\nabla \boldsymbol{u}^{R,H} - \boldsymbol{R}(\nabla \boldsymbol{u}^{R,H})) : \boldsymbol{E}^{-1} : (\boldsymbol{E}:\nabla \boldsymbol{u}^{R,H} - \boldsymbol{R}(\nabla \boldsymbol{u}^{R,H}))\, \mathrm{d}\boldsymbol{x}}_{\zeta^2(\mathbf{u}^{R,H})}$$
$$- \underbrace{\int_{\Omega} (\boldsymbol{E}:\nabla \boldsymbol{u}^{R} - \boldsymbol{R}(\nabla \boldsymbol{u}^{R})) : \boldsymbol{E}^{-1} : (\boldsymbol{E}:\nabla \boldsymbol{u}^{R} - \boldsymbol{R}(\nabla \boldsymbol{u}^{R}))\, \mathrm{d}\boldsymbol{x}}_{\zeta^2(\boldsymbol{u}^{R})}.$$

This is the error in using the discrete version of $\zeta(\boldsymbol{u}^{\mathrm{R}})$, $\zeta(\boldsymbol{u}^{R,H})$. We note that, in general, the sign of $\Lambda(\boldsymbol{u}^{R}, \boldsymbol{u}^{R,H})$ is indefinite.

Substituting these quantities into the decomposition error bound, we have, by direct expansion

$$\underbrace{\psi^2(\tilde{\boldsymbol{u}}^{R,ID,H,h}, \boldsymbol{u}^{R,H}, \zeta(\boldsymbol{u}^{R,H}))}_{\text{computed error estimate}} = \psi^2(\tilde{\boldsymbol{u}}^{R,ID} + \mathbf{e}^{h} + \mathbf{e}^{H-h}, \boldsymbol{u}^{R} + \mathbf{e}^{R,H}, \zeta(\boldsymbol{u}^{R,H}))$$

$$= \psi^2(\tilde{\boldsymbol{u}}^{R,ID}, \boldsymbol{u}^{R}, \zeta(\boldsymbol{u}^{R})) + \mathscr{B}(\mathbf{e}^{h}, \mathbf{e}^{h})$$

$$\underbrace{+2(\mathscr{B}(\tilde{\boldsymbol{u}}^{R,ID}, \mathbf{e}^{h}) - \mathscr{F}(\mathbf{e}^{h}))}_{\Sigma_{K=1}^{N}\{\mathscr{B}_K(\tilde{\boldsymbol{u}}_K^{R,ID}, \mathbf{e}_K^{h}) - \mathscr{F}_K(\mathbf{e}_K^{h})\} = 0}$$

$$+2\mathscr{J}(\mathbf{e}^{H-h}) + \mathscr{B}(\tilde{\boldsymbol{u}}^{R,ID}, \mathbf{e}^{R,H}) + \mathscr{B}(\mathbf{e}^{R,H}, \mathbf{e}^{h}) - 2\mathscr{J}(\mathbf{e}^{R,H})$$

$$-2\mathscr{B}(\boldsymbol{u}^{R}, \mathbf{e}^{R,H}) + \Lambda(\boldsymbol{u}^{R}, \boldsymbol{u}^{R,H}) = \underbrace{\psi^2(\tilde{\boldsymbol{u}}^{R,ID}, \boldsymbol{u}^{R}, \zeta(\boldsymbol{u}^{R}))}_{\text{decoupling error bound}}$$

$$\underbrace{+\sum_{K=1}^{N} \|\tilde{\boldsymbol{u}}_K^{R,ID,h} - \tilde{\boldsymbol{u}}_K^{R,ID}\|_{E(\Omega_K)}^2}_{\text{subdomain discretization error}}$$

$$+\text{terms of indefinite sign that are zero if } \mathbf{e}^{R,H} = \mathbf{0}.$$

Following the same procedure, but employing the applied internal traction approach and the corresponding complementary variational principles, we have

$$\underbrace{\Phi^2(\tilde{\boldsymbol{\sigma}}^{L,IS,H,h}, \boldsymbol{\sigma}^{L,H}, \beta(\boldsymbol{\sigma}^{L,H}))}_{\text{computed error estimate}} = \underbrace{\Phi^2(\tilde{\boldsymbol{\sigma}}^{L,IS}, \boldsymbol{\sigma}^{L}, \beta(\boldsymbol{\sigma}^{L}))}_{\text{decoupling error bound}} + \underbrace{\sum_{K=1}^{N} \|\tilde{\boldsymbol{\sigma}}_K^{L,IS,h} - \tilde{\boldsymbol{\sigma}}_K^{L,IS}\|_{E-1(\Omega_K)}^2}_{\text{subdomain discretization error}}$$

$$+\text{terms of indefinite sign that are zero if } \mathbf{e}^{R,H} = \mathbf{0}.$$

These expressions indicate that, in the calculation of the regularized decoupling solution, the discretization error should be made as small as possible, otherwise it pollutes all subsequent error estimates, making them unreliable. When there is no discretization error in the regularized decoupling solution, the 'extra' indefinite terms vanish, and we obtain the following orthogonal decomposition

$$\underbrace{\psi^2(\tilde{\boldsymbol{u}}^{R,ID,h}, \boldsymbol{u}^{R}, \zeta(\boldsymbol{u}^{R}))}_{\text{calculated}} = \underbrace{\psi^2(\tilde{\boldsymbol{u}}^{R,ID}, \boldsymbol{u}^{R}, \zeta(\boldsymbol{u}^{R}))}_{\text{decoupling error bound}} + \underbrace{\sum_{K=1}^{N} \|\tilde{\boldsymbol{u}}_K^{R,ID,h} - \tilde{\boldsymbol{u}}_K^{R,ID}\|_{E(\Omega_K)}^2}_{\text{subdomain discretization error}}$$

$$\geqslant \|\boldsymbol{u} - \tilde{\boldsymbol{u}}^{R,ID}\|_{E(\Omega)}^2 + \sum_{K=1}^{N} \|\tilde{\boldsymbol{u}}_K^{R,ID,h} - \tilde{\boldsymbol{u}}_K^{R,ID}\|_{E(\Omega)}^2 = \|\boldsymbol{u} - \tilde{\boldsymbol{u}}^{R,ID,h}\|_{E(\Omega)}^2 \tag{5}$$

where the last equality comes directly from the PMPE and

$$\underbrace{\Phi^2(\tilde{\boldsymbol{\sigma}}^{R,ID,h},\boldsymbol{\sigma}^L,\beta(\boldsymbol{\sigma}^L))}_{\text{calculated}} = \underbrace{\Phi^2(\tilde{\boldsymbol{\sigma}}^{L,IS},\boldsymbol{\sigma}^L,\beta(\boldsymbol{\sigma}^L))}_{\text{decoupling error bound}} + \underbrace{\sum_{K=1}^{N}\|\tilde{\boldsymbol{\sigma}}_K^{L,IS,h}-\tilde{\boldsymbol{\sigma}}_K^{L,IS}\|^2_{E^{-1}(\Omega_K)}}_{\text{subdomain discretization error}}$$

$$\geqslant \|\boldsymbol{\sigma}-\tilde{\boldsymbol{\sigma}}^{L,IS}\|^2_{E^{-1}(\Omega)} + \sum_{K=1}^{N}\|\tilde{\boldsymbol{\sigma}}_K^{L,IS,h}-\tilde{\boldsymbol{\sigma}}_K^{L,IS}\|^2_{E^{-1}(\Omega)}$$

$$= \|\boldsymbol{\sigma}-\tilde{\boldsymbol{\sigma}}^{L,IS,h}\|^2_{E^{-1}(\Omega)}, \tag{6}$$

where the last equality comes from the PMCPE. We now show that these general expressions collapse to relatively simple forms in an important application.

4. A special case: application to a representative volume element

The computation of effective properties of heterogeneous materials involve the solution of boundary value problems posed over statistically representative volume element domains. In many cases such simulations are quite computationally complex. For examples see Suquet (1987). As a special application we now apply the presented decomposition process, and error bounds, to this class of problems.

4.1. Background

In order to determine an effective macroscopic linear elasticity tensor, $\boldsymbol{E}^*$, a relation between averages, $\langle\boldsymbol{\sigma}\rangle_\Omega = \boldsymbol{E}^*\colon\langle\boldsymbol{\varepsilon}\rangle_\Omega$, must be computed, where $\langle\cdot\rangle_\Omega \stackrel{\text{def}}{=} (1/|\Omega|)\int_\Omega \cdot\, \mathrm{d}\boldsymbol{x}$, and where $\boldsymbol{\sigma}$ and $\boldsymbol{\varepsilon}$ are the stress and strain fields within a statistically representative volume element (RVE) with volume $|\Omega|$. Loosely speaking, an RVE is a theoretical structure that is small enough that it can be considered as a material point with respect to the size of the domain under analysis, but large enough to be a statistically representative sample of the microstructure (Fig. 3). Here we assume that at least one choice of the RVE is possible. For more details see Kröner (1972) or Suquet (1987).

In general, $\boldsymbol{E}^*$ is not a material property, it is a relation between averages. If $\langle\boldsymbol{\sigma}\rangle_\Omega$ and $\langle\boldsymbol{\varepsilon}\rangle_\Omega$ are such that

$$\underbrace{\langle\boldsymbol{\sigma}\colon\boldsymbol{\varepsilon}\rangle_\Omega}_{\text{micro energy}} = \underbrace{\langle\boldsymbol{\sigma}\rangle_\Omega\colon\langle\boldsymbol{\varepsilon}\rangle_\Omega}_{\text{macro energy}} \tag{7}$$

then there exist bounds on $\boldsymbol{E}^*$,

$$\underbrace{\langle\boldsymbol{E}^{-1}\rangle_\Omega^{-1}}_{\text{Reuss}} \leqslant \boldsymbol{E}^* \leqslant \underbrace{\langle\boldsymbol{E}\rangle_\Omega}_{\text{Voigt}},$$

where this inequality means that the eigenvalues of the tensors $\boldsymbol{E}^* - \langle\boldsymbol{E}^{-1}\rangle_\Omega^{-1}$ and $\langle\boldsymbol{E}\rangle_\Omega - \boldsymbol{E}^*$ are non-negative. This result was proven by Hill (1952). These bounds are commonly known as the Reuss–Voigt bounds, for the following historical reasons. Voigt (1889), assumed that the strain field within a sample of aggregate of polycrystalline material, was uniform (constant), under

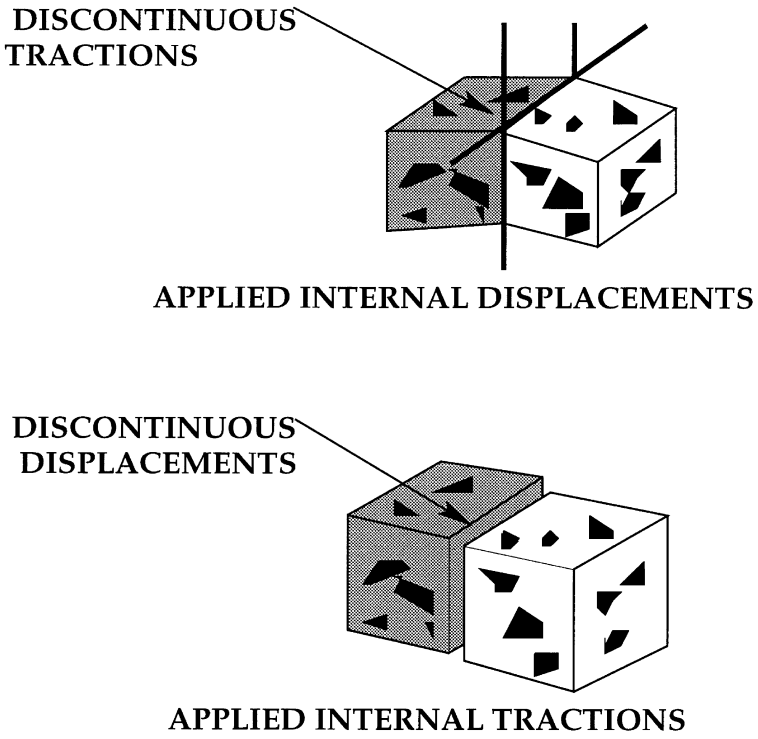

Fig. 2. The consequences of the two domain decomposition approaches.

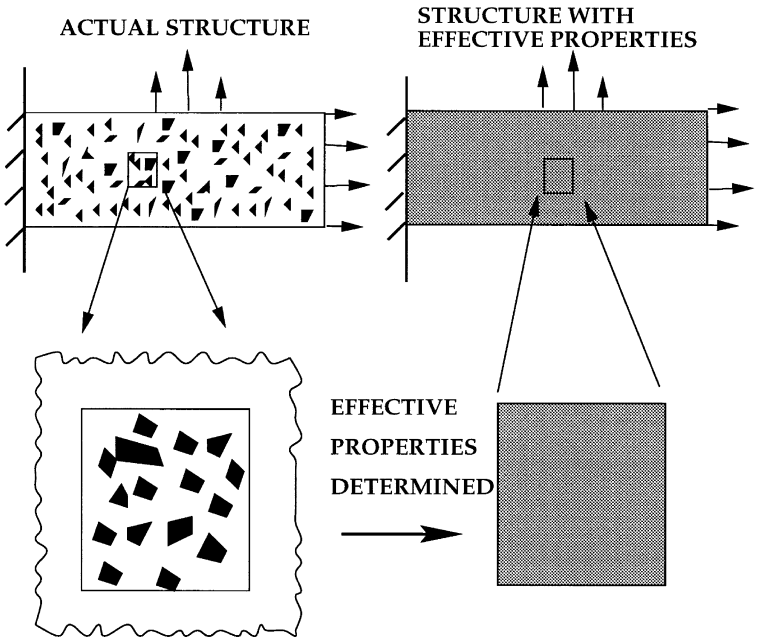

Fig. 3. The standard use of the RVE concept.

uniform strain exterior loading. If the Voigt field is assumed within the RVE, then $\langle \boldsymbol{E} \rangle_\Omega$ results as the effective property. The dual assumption was made by Reuss (1929), who approximated the stress fields within the aggregate of polycrystalline material as uniform (constant), under uniform stress loading. If the Reuss field is assumed within the RVE, then the effective property becomes $\langle \boldsymbol{E}^{-1} \rangle_\Omega^{-1}$. Equality is attained in the above bounds when the Reuss or Voigt assumptions hold, respectively. These conditions are important in characterizing certain aspects of the method presented in this work, and are discussed in the next section.

4.2. Special forms of the general error bounds for uniform boundary conditions

The relation in Box (7), often referred in the literature as Hill's condition, can be realized in several ways. A special class of fields that fall under Hill's condition are those produced in bodies with applied boundary data of the following form: (1) pure displacements in the form $\boldsymbol{u}|_{\partial\Omega} = \mathscr{S} \cdot \boldsymbol{x}$ or (2) pure tractions in the form $\boldsymbol{t}|_{\partial\Omega} = \mathscr{T} \cdot \boldsymbol{n}$; where $\mathscr{S}$ and $\mathscr{T}$ are constant strain and stress tensors, respectively. For obvious reasons, these types of boundary conditions are known as 'uniform'. It can be easily shown that under uniform conditions, with no body forces, that for case (1) $\langle \boldsymbol{\varepsilon} \rangle_\Omega = \mathscr{S}$, and for the case (2) $\langle \boldsymbol{\sigma} \rangle_\Omega = \mathscr{T}$. Under these loading conditions the solution to the regularized decoupling boundary value problem used in the decomposition process is trivial to calculate: (1) $\boldsymbol{u}|_{\partial\Omega} = \mathscr{S} \cdot \boldsymbol{x} \Rightarrow \boldsymbol{\varepsilon}^R = \mathscr{S}$ or (2) $\boldsymbol{t}|_{\partial\Omega} = \mathscr{T} \cdot \boldsymbol{n} \Rightarrow \boldsymbol{\sigma}^L = \mathscr{T}$. These conditions allow the general error bounds derived in this paper to collapse into forms which imply an effective (macroscopic) material ordering relationship. In particular, the collapsed forms of the decomposition error bounds imply bounds on effective material properties.

4.3. The applied internal displacement case

The following analysis is valid for any body, regardless whether it is an RVE or not. Throughout we use the symbol $\boldsymbol{E}^*$ to signify a relation between averages, $\langle \boldsymbol{\sigma} \rangle_\Omega = \boldsymbol{E}^* : \langle \boldsymbol{\varepsilon} \rangle_\Omega$, which is not necessarily an effective property. It is trivial to show that if $\boldsymbol{u}|_{\partial\Omega} = \mathscr{S} \cdot \boldsymbol{x}$, $\boldsymbol{f} = \boldsymbol{0}$, and if $\boldsymbol{R}$ is an admissible constant linear elasticity tensor, then with the following definitions

$$\langle \tilde{\boldsymbol{\sigma}}^{R,ID,h} \rangle_{\Omega_K} \stackrel{\text{def}}{=} \tilde{\boldsymbol{E}}^{*,R,ID,h}_K : \langle \tilde{\boldsymbol{\varepsilon}}^{R,ID,h} \rangle_{\Omega_K}, \quad \langle \tilde{\boldsymbol{\sigma}}^{R,ID} \rangle_{\Omega_K} \stackrel{\text{def}}{=} \tilde{\boldsymbol{E}}^{*,R,ID}_K : \langle \tilde{\boldsymbol{\varepsilon}}^{R,ID} \rangle_{\Omega_K},$$

$$\tilde{\boldsymbol{E}}^{*,R,ID,h} \stackrel{\text{def}}{=} \sum_{K=1}^{N} \tilde{\boldsymbol{E}}^{*,R,ID,h}_K \frac{|\Omega_K|}{|\Omega|}, \quad \tilde{\boldsymbol{E}}^{*,R,ID} \stackrel{\text{def}}{=} \sum_{K=1}^{N} \tilde{\boldsymbol{E}}^{*,R,ID}_K \frac{|\Omega_K|}{|\Omega|}, \tag{8}$$

we have

$$\begin{aligned}
&\|\boldsymbol{u} - \tilde{\boldsymbol{u}}^{R,ID}\|^2_{E(\Omega)} = \mathscr{S} : (\tilde{\boldsymbol{E}}^{*,R,ID} - \boldsymbol{E}^*) : \mathscr{S} |\Omega|,\\
&\|\boldsymbol{u} - \tilde{\boldsymbol{u}}^{R,ID,h}\|^2_{E(\Omega)} = \mathscr{S} : (\tilde{\boldsymbol{E}}^{*,R,ID,h} - \boldsymbol{E}^*) : \mathscr{S} |\Omega|,\\
&\|\boldsymbol{u}^{R,ID,h} - \tilde{\boldsymbol{u}}^{R,ID}\|^2_{E(\Omega)} = \mathscr{S} : (\tilde{\boldsymbol{E}}^{*,R,ID,h} - \tilde{\boldsymbol{E}}^{*,R,ID}) : \mathscr{S} |\Omega|,\\
&\zeta^2(\boldsymbol{u}^R) = \mathscr{S} : (\langle \boldsymbol{E} \rangle_\Omega - 2\boldsymbol{R} + \boldsymbol{R} : \langle \boldsymbol{E}^{-1} \rangle_\Omega : \boldsymbol{R}) : \mathscr{S} |\Omega|,\\
&\Psi^2(\tilde{\boldsymbol{u}}^{R,ID,h}, \boldsymbol{u}^R, \zeta(\boldsymbol{u}^R)) = \mathscr{S} : (\tilde{\boldsymbol{E}}^{*,R,ID,h} - 2\boldsymbol{R} + \boldsymbol{R} : \langle \boldsymbol{E}^{-1} \rangle_\Omega : \boldsymbol{R}) : \mathscr{S} |\Omega|.
\end{aligned} \tag{9}$$

It is emphasized that, under these conditions, the actual errors are independent of $\boldsymbol{R}$. However, the bounds on the error are not. Therefore, since $\boldsymbol{R}$ is a free tensorial parameter, we can minimize the error bound with it, to yield

$$\frac{\partial \Psi^2}{\partial \boldsymbol{R}} = -\mathscr{S}:(2\boldsymbol{I}-2\langle \boldsymbol{E}^{-1}\rangle_\Omega : \boldsymbol{R}):\mathscr{S}|\Omega| = 0 \Rightarrow \boldsymbol{R} = \langle \boldsymbol{E}^{-1}\rangle_\Omega^{-1},$$

$$\Rightarrow \Psi^2(\tilde{\boldsymbol{u}}^{R,ID,h}, \boldsymbol{u}^R, \zeta(\boldsymbol{u}^R)) = \mathscr{S}:(\tilde{\boldsymbol{E}}^{*,R,ID,h} - \langle \boldsymbol{E}^{-1}\rangle_\Omega^{-1}):\mathscr{S}|\Omega|,$$

$$\Rightarrow \zeta^2(\boldsymbol{u}^R) = \mathscr{S}:(\langle \boldsymbol{E}\rangle_\Omega - \langle \boldsymbol{E}^{-1}\rangle_\Omega^{-1}):\mathscr{S}|\Omega|. \tag{10}$$

It is not surprising that the optimal decoupling material for the error bound is $\langle \boldsymbol{E}^{-1}\rangle_\Omega^{-1}$, the Reuss (approximate effective) material. Loosely speaking, this choice, among possible effective materials contained within the Reuss–Voigt inequalities, is the 'softest' possible effective material, for a fixed microstructure. This choice to minimize the error bound has some intuitive basis. If one recalls the first two lines of Equation set (1) and Fig. 2, it is clear that a 'soft' material allows the inter-subdomain tractions to match more closely than a 'harder' decoupling material.

4.3.1. An implied effective material ordering

Using the orthogonal decomposition in Box (5), we obtain

$$\underbrace{\mathscr{S}:(\tilde{\boldsymbol{E}}^{*,R,ID,h} - \boldsymbol{E}^*):\mathscr{S}|\Omega|}_{\|\boldsymbol{u}-\tilde{\boldsymbol{u}}^{R,ID,h}\|^2_{E(\Omega)}} = \underbrace{\mathscr{S}:(\tilde{\boldsymbol{E}}^{*,R,ID} - \boldsymbol{E}^*):\mathscr{S}|\Omega|}_{\|\boldsymbol{u}-\tilde{\boldsymbol{u}}^{R,ID}\|^2_{E(\Omega)}} + \underbrace{\sum_{K=1}^{N} \|\tilde{\boldsymbol{u}}_K^{R,ID,h} - \tilde{\boldsymbol{u}}_K^{R,ID}\|^2_{E(\Omega)}}_{\mathscr{S}:(\tilde{\boldsymbol{E}}^{*,R,ID,h} - \tilde{\boldsymbol{E}}^{*,R,ID}):\mathscr{S}|\Omega|}$$

and

$$\underbrace{\mathscr{S}:(\tilde{\boldsymbol{E}}^{*,R,ID,h} - \langle \boldsymbol{E}^{-1}\rangle_\Omega^{-1}):\mathscr{S}|\Omega|}_{\Psi^2(\tilde{\boldsymbol{u}}^{R,ID,h},\boldsymbol{u}^R,\zeta(\boldsymbol{u}^R))} = \underbrace{\mathscr{S}:(\tilde{\boldsymbol{E}}^{*,R,ID} - \langle \boldsymbol{E}^{-1}\rangle_\Omega^{-1}):\mathscr{S}}_{\Psi^2(\tilde{\boldsymbol{u}}^{R,ID},\boldsymbol{u}^R,\zeta(\boldsymbol{u}^R))} + \underbrace{\sum_{K=1}^{N} \|\tilde{\boldsymbol{u}}_K^{R,ID,h} - \tilde{\boldsymbol{u}}_K^{R,ID}\|^2_{E(\Omega)}}_{\mathscr{S}:(\tilde{\boldsymbol{E}}^{*,R,ID,h} - \tilde{\boldsymbol{E}}^{*,R,ID}):\mathscr{S}|\Omega|}$$

$$\leqslant \underbrace{\mathscr{S}:(\langle \boldsymbol{E}\rangle_\Omega - \langle \boldsymbol{E}^{-1}\rangle_\Omega^{-1}):\mathscr{S}|\Omega|}_{\zeta^2(\boldsymbol{u}^R)} + \underbrace{\sum_{K=1}^{N} \|\tilde{\boldsymbol{u}}_K^{R,ID,h} - \tilde{\boldsymbol{u}}_K^{R,ID}\|^2_{E(\Omega)}}_{\mathscr{S}:(\tilde{\boldsymbol{E}}^{*,R,ID,h} - \tilde{\boldsymbol{E}}^{*,R,ID}):\mathscr{S}|\Omega|}.$$

The above immediately imply the following regularized material ordering:

$$\langle \boldsymbol{E}^{-1}\rangle_\Omega^{-1} \leqslant \boldsymbol{E}^* \leqslant \tilde{\boldsymbol{E}}^{*,R,ID} \leqslant \tilde{\boldsymbol{E}}^{*,R,ID,h},$$

$$\mathscr{S}:(\tilde{\boldsymbol{E}}^{*,R,ID,h} - \langle \boldsymbol{E}\rangle):\mathscr{S}|\Omega| \leqslant \sum_{K=1}^{N} \|\tilde{\boldsymbol{u}}_K^{R,ID,h} - \tilde{\boldsymbol{u}}_K^{R,ID}\|^2_{E(\Omega)}. \tag{11}$$

The last expression in Equation set (11) is also a lower bound on the numerical error in the subdomain computations.

4.4. The applied internal traction case

As in the previous case, the following analysis is valid for any body, regardless whether it is an RVE or not. Throughout we use the symbol $\boldsymbol{C}^*$ to signify a relation between averages, $\langle \boldsymbol{\varepsilon} \rangle_\Omega = \boldsymbol{C}^* : \langle \boldsymbol{\sigma} \rangle_\Omega$, which is not necessarily an effective property. For the applied internal traction case, the procedure is identical. If $\boldsymbol{R}$ is an admissible constant linear elasticity tensor ($\boldsymbol{L} = \boldsymbol{R}^{-1}$), and $\boldsymbol{t}|_{\partial\Omega} = \mathscr{T} \cdot \boldsymbol{n}, \boldsymbol{f} = \boldsymbol{0}$, then defining

$$\langle \tilde{\boldsymbol{\varepsilon}}^{L,IS,h} \rangle_{\Omega_K} = \tilde{\boldsymbol{E}}^{*\,-1,L,IS,h}_{K} : \langle \tilde{\boldsymbol{\sigma}}^{L,IS,h} \rangle_{\Omega_K}, \quad \langle \tilde{\boldsymbol{\varepsilon}}^{L,IS} \rangle_{\Omega_K} = \tilde{\boldsymbol{E}}^{*\,-1,IS}_{K} : \langle \tilde{\boldsymbol{\sigma}}^{L,IS} \rangle_{\Omega_K},$$

$$\tilde{\boldsymbol{E}}^{*\,-1,L,IS,h} \stackrel{\text{def}}{=} \sum_{K=1}^{N} \tilde{\boldsymbol{E}}^{*\,-1,L,IS,h}_{K} \frac{|\Omega_K|}{|\Omega|}, \quad \tilde{\boldsymbol{E}}^{*\,-1,IS} \stackrel{\text{def}}{=} \sum_{K=1}^{N} \tilde{\boldsymbol{E}}^{*\,-1,IS}_{K} \frac{|\Omega_K|}{|\Omega|}, \tag{12}$$

we have

$$\begin{aligned}
&\|\boldsymbol{\sigma} - \tilde{\boldsymbol{\sigma}}^{L,IS}\|^2_{E^{-1}(\Omega)} = \mathscr{T} : (\tilde{\boldsymbol{E}}^{*\,-1,IS} - \boldsymbol{C}^*) : \mathscr{T} |\Omega|,\\
&\|\boldsymbol{\sigma} - \tilde{\boldsymbol{\sigma}}^{L,IS,h}\|^2_{E^{-1}(\Omega)} = \mathscr{T} : (\tilde{\boldsymbol{E}}^{*\,-1,L,IS,h} - \boldsymbol{C}^*) : \mathscr{T} |\Omega|,\\
&\|\tilde{\boldsymbol{\sigma}}^{L,IS,h} - \tilde{\boldsymbol{\sigma}}^{L,IS}\|^2_{E^{-1}(\Omega)} = \mathscr{T} : (\tilde{\boldsymbol{E}}^{*\,-1,L,IS,h} - \tilde{\boldsymbol{E}}^{*\,-1,IS}) : \mathscr{T} |\Omega|,\\
&\beta^2(\boldsymbol{\sigma}^L) = \mathscr{T} : (\langle \boldsymbol{E}^{-1} \rangle_\Omega - 2\boldsymbol{R}^{-1} + \boldsymbol{R}^{-1} : \langle \boldsymbol{E}^{-1} \rangle_\Omega : \boldsymbol{R}^{-1}) : \mathscr{T} |\Omega|,\\
&\Phi^2(\tilde{\boldsymbol{\sigma}}^{L,IS,h}, \boldsymbol{\sigma}^L, \beta(\boldsymbol{\sigma}^L)) = \mathscr{T} : (\tilde{\boldsymbol{E}}^{*\,-1,L,IS,h} - 2\boldsymbol{R}^{-1} + \boldsymbol{R}^{-1} : \langle \boldsymbol{E}^{-1} \rangle_\Omega : \boldsymbol{R}^{-1}) : \mathscr{T} |\Omega|.
\end{aligned} \tag{13}$$

As in the applied internal displacement case, the actual errors are independent of the regularized decoupling material, in this case $\boldsymbol{R}^{-1}$. However, as before, the error bounds are not. Therefore, since $\boldsymbol{R}^{-1}$ is a free tensorial parameter, we can minimize the error bound with it, to obtain

$$\begin{aligned}
&\frac{\partial \Phi^2}{\partial \boldsymbol{R}^{-1}} = -\mathscr{T} : (2\boldsymbol{I} - 2\langle \boldsymbol{E} \rangle_\Omega : \boldsymbol{R}^{-1}) \mathscr{T} |\Omega| = 0 \Rightarrow \boldsymbol{R} = \langle \boldsymbol{E} \rangle_\Omega,\\
&\quad \Rightarrow \Phi^2(\tilde{\boldsymbol{\sigma}}^{L,IS,h}, \boldsymbol{\sigma}^L, \beta(\boldsymbol{\sigma}^L)) = \mathscr{T} : (\tilde{\boldsymbol{E}}^{*\,-1,L,IS,h} - \langle \boldsymbol{E} \rangle_\Omega^{-1}) : \mathscr{T} |\Omega|,\\
&\quad \Rightarrow \beta^2(\boldsymbol{\sigma}^L) = \mathscr{T} : (\langle \boldsymbol{E}^{-1} \rangle_\Omega - \langle \boldsymbol{E} \rangle_\Omega^{-1}) : \mathscr{T} |\Omega|.
\end{aligned} \tag{14}$$

The optimal regularized decoupling material to minimize the error bound is $\langle \boldsymbol{E} \rangle_\Omega$, the Voigt (approximate effective) material. This choice, among possible effective materials contained in the Reuss–Voigt inequalities, is the 'hardest' possible effective material. As the last two lines of Equation set (1) and Fig. 2 imply, a 'hard' material allows the regularized displacement to be minimized, forcing the inter-subdomain displacement jumps to be minimized.

4.4.1. An implied effective material ordering

The above relations immediately imply, via the orthogonality conditions of Equation set (6), the following effective material ordering for the applied internal traction case

$$\tilde{\boldsymbol{E}}^{*-1,L,IS,h} \geqslant \tilde{\boldsymbol{E}}^{*-1,L,IS} \geqslant \boldsymbol{C}^{*} \geqslant \langle \boldsymbol{E} \rangle_{\Omega}^{-1},$$

$$\mathscr{T}:(\tilde{\boldsymbol{E}}^{*-1,L,IS,h} - \langle \boldsymbol{E}^{-1} \rangle_{\Omega}):\mathscr{T}|\Omega| \leqslant \sum_{K=1}^{N} \|\tilde{\boldsymbol{\sigma}}_{K}^{L,IS,h} - \boldsymbol{\sigma}_{K}^{L,IS}\|^{2}_{E^{-1}(\Omega)}. \tag{15}$$

The second expression in Equation set (15) is a lower bound on the numerical error in the subdomain calculations.

In the ideal case that there is no numerical error in the subdomain computations, and the body is an RVE ($\boldsymbol{E}^{*} = \boldsymbol{C}^{*-1}$), then the preceding analysis yields the following two sided ordering of approximate effective materials,

$$\langle \boldsymbol{E}^{-1} \rangle_{\Omega}^{-1} \leqslant (\tilde{\boldsymbol{E}}^{*-1,L,IS})^{-1} \leqslant \boldsymbol{E}^{*} \leqslant \tilde{\boldsymbol{E}}^{*,R,ID} \leqslant \langle \boldsymbol{E} \rangle_{\Omega}. \tag{16}$$

4.5. Comments

It is important to note that the general results presented earlier in the analysis, in particular the relations in Box (4), are bounds on the error in the approximate microfields under nonuniform loading which, in the special case of uniform external loading, collapse into forms which imply an ordering of approximate effective material properties, expressed in Equation set (16). The results in Equation set (16) coincide with those published by Huet (1990). It is important to emphasize that the goal of Huet was to bound the effective material properties, while in this work the goal was to approximate the solution to a boundary value problem describing the deformation of a body with microstructure, under arbitrary loading. Here the effective property ordering is a by-product of the error analysis on the approximate microstructural fields. The fact that the results coincide for the special case of uniform boundary conditions is not surprising, since both methods are based on the same minimum principles, the PMPE and the PMCPE. However, Huet's analysis was restricted to uniform exterior loading, and did not employ the use of a regularized decoupling solution, which is central to the ability to analyze cases with nonuniform exterior loading.

The decomposition error bounds can collapse even further. If the exterior loading is of linear displacement type, the subdomain boundaries are the material interfaces and the subdomains contain no material heterogeneities (Fig. 4), then the applied internal displacement method produces a field which coincides with the Voigt field. Similarly, if the exterior loading is of uniform traction type, the subdomain partitions are the material interfaces and the subdomains contain no material heterogeneities (Fig. 4), then the applied internal traction approach produces a field which coincides with the Reuss field.

5. Summary

In this work a method of model reduction, or material substructuring, via a nonoverlapping domain decomposition, has been developed. Special cases of the method have been determined previously in Zohdi et al. (1996) and in Oden and Zohdi (1997) for the applied internal displacement case. In particular, in Oden and Zohdi (1997), error bounds were developed for linear decoupling materials, neglecting the discretization error, and were used as a basis for large-scale numerical simulations of bodies with particulate composition microstructure. The error bounds were used to

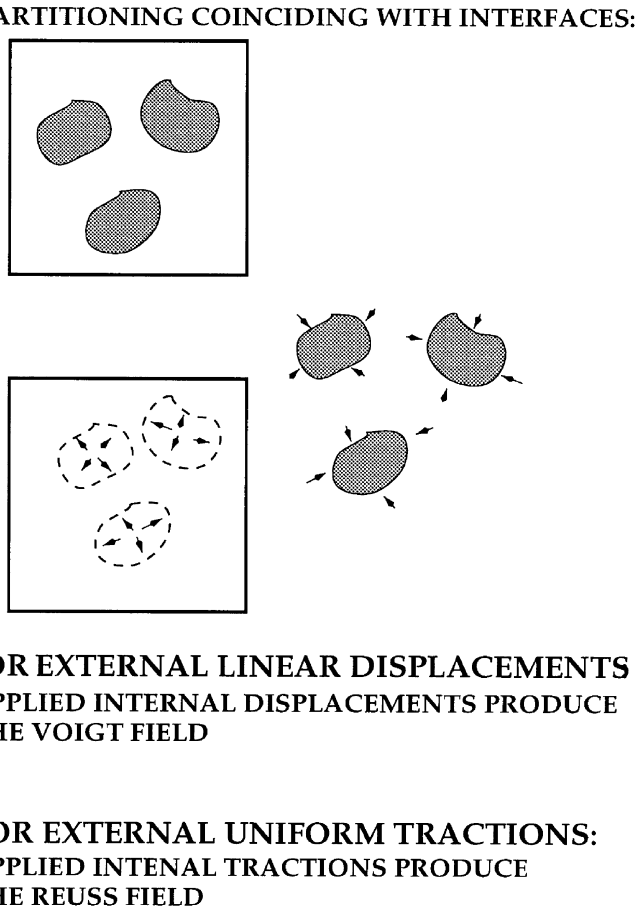

Fig. 4. Special cases of the domain decomposition process for uniform external loading.

adaptively select the subdomain partitioning (the subdomain sizes). In this work we have presented the following extensions to those works: (1) the development of error bounds using nonlinear decoupling materials, (2) the development of the (dual) applied internal traction approach and error bounds, (3) the consideration of the effects of discretization error on the bounds and finally (4) the important application to a representative volume element structure.

In view of the authors, the presented method is a way to augment existing techniques of analysis. Purposely, we did not attach it to any specific numerical method. Usually, the operation counts to solve a discrete system with N discrete unknowns are between N^2 and N^3, and therefore by breaking it into M decoupled subproblems, the number of operation counts are approximately between $M \times (N/M)^2 = N^2/M$ and $M \times (N/M)^3 = N^3/M^2$. The memory requirements which, with most discretization methods, scale in a similar manner, can also be dramatically reduced since one subdomain can be stored, the subproblem solved, and the data overwritten. This is especially attractive to a researcher using a single workstation or PC. Furthermore, these computations can

be performed in a very fast and efficient manner, since the subdomain problems are completely decoupled and, because no interprocessor communication is required, trivially parallelizable.

Finally, there are several further comments/improvements/extensions that can be made pertaining to the method and its implementation, and they are as follows:

- From a computational point of view, the applied internal displacement approach is usually more attractive than the applied internal traction approach, since the rigid motions, present in the latter approach, must be controlled for each subdomain. Also, most numerical methods are based on discretization of displacement-based variational formulations. However, there are efficient means to construct statically admissible fields needed in using complementary principles. For details see Ladeveze and Leguillon (1983).
- If the subdomain partitioning intersects a material interface, then, in general, a singularity in stress will occur. To avoid this, special care must be taken when selecting a subdomain partitioning.
- If the estimated error is too high, then approximate solutions can be improved after the first decoupled solution process, by employing standard alternating domain decomposition methods of overlapping or nonoverlapping type (see Le Tallec (1994)). Essentially these methods can be used to balance the jumps in the tractions at the inter-subdomain boundaries, for the applied internal displacement approach, and to balance the jumps in the displacements at the inter-subdomain boundaries for the applied internal traction case.
- Clearly, as the subdomains get larger, and less in number, the decoupling error decreases and tends to zero. However, the subdomain problems become harder to solve numerically, and, correspondingly, the numerical error grows. A primary future interest should focus on optimizing the choice of the subdomain partitioning to minimize the total error, consisting of the numerical and decoupling errors, for the computational resources available.
- A well known relation, valid for arbitrary admissible exterior loading conditions, is $\mathscr{J}(\boldsymbol{u})+\mathscr{K}(\boldsymbol{\sigma})=0$, implies the following,

$$2(\mathscr{J}(\boldsymbol{u}^R)+\mathscr{K}(\boldsymbol{\sigma}^L)) = \|\boldsymbol{u}-\boldsymbol{u}^R\|^2_{E(\Omega)}+\|\boldsymbol{\sigma}-\boldsymbol{\sigma}^L\|^2_{E^{-1}(\Omega)},$$

$$2(\mathscr{J}(\tilde{\boldsymbol{u}}^{R,ID})+\mathscr{K}(\tilde{\boldsymbol{\sigma}}^{L,IS})) = \|\boldsymbol{u}-\tilde{\boldsymbol{u}}^{R,ID}\|^2_{E(\Omega)}+\|\boldsymbol{\sigma}-\tilde{\boldsymbol{\sigma}}^{L,IS}\|^2_{E^{-1}(\Omega)}.$$

  Therefore, there exists the ability to estimate the exact error of the two approaches. Unfortunately, the direct use of these expressions for error estimation poses some difficulties, since they do not characterize the quality of either solution separately. However, these relations are useful in developing lower bounds, for each measure separately, following similar approaches as found in this paper.
- To determine the internal microfields, further reduction of the computational effort can be achieved employing the following local sensitivity properties, which are directly derived by application of the results in Equation sets (2) and (3) to an individual subdomain (using the regularized solution as interior subdomain interface data):

$$\|\tilde{\boldsymbol{u}}^{R,ID}_K-\boldsymbol{u}^R_K\|_{E(\Omega_K)} \leqslant \zeta_K(\boldsymbol{u}^R),$$

$$\|\tilde{\boldsymbol{\sigma}}^{L,IS}_K-\boldsymbol{\sigma}^L_K\|_{E^{-1}(\Omega_K)} \leqslant \beta_K(\boldsymbol{\sigma}^L). \tag{17}$$

  Notice for subdomains where ζ_K or β_K is small, there is little predicted difference in the regularized

decoupling solution and subdomain solution. Therefore, there exists the ability to select only those subdomains with ζ_K's or β_K's that are above a certain tolerance for the subdomain solution process, retaining the regularized decoupling solution otherwise. The first expression in Equation set (17) has been developed earlier, for the linear decoupling materials, in Zohdi et al. (1996) and used in Oden and Zohdi (1997) to reduce computational effort by solving only those subdomains which are identified as sensitive (above a preset tolerance) to the microstructure.

- If possible, the method, and error estimates, should be extended to boundary value formulations describing time dependent, inelastic finite deformations, on both the micro- and macro-scales. This is a topic of current research of the authors. Obviously, in its present form, the method can be directly applied, without modification, to a linearized load or time increment.

Acknowledgement

The authors thank Professor Christian Huet and Professor Gregory Rodin for their constructive comments during the writing of this paper.

References

Hill, R., 1952. The elastic behaviour of a crystalline aggregate. Proc. Phys. Soc. Lond. A65, 349–354.

Huet, C., 1990. Application of variational concepts to size effects in elastic heterogeneous bodies. Journal of the Mechanics and Physics of Solids 38, 813–841.

Kröner, E., 1972. Statistical Continuum Mechanics. CISM Lecture Notes, Springer-Verlag, 92.

Ladeveze, P., Leguillon, D., 1983. Error estimate procedure in the finite element method and applications. SIAM J. Numerical Anal. 20, 485–509.

Le Tallec, P., 1994. Domain decomposition methods in computation mechanics. Computational Mechanics Advances 1, 121–220.

Oden, J.T., Zohdi, T.I., 1997. Analysis and adaptive modeling of highly heterogeneous elastic structures. Computer Methods in Applied Mechanics and Engineering 148, 367–391.

Reuss, A., 1929. Berechnung der Fliessgrenze von Mischkristallen auf Grund der Plastizitätsbedingung für Einkrisalle. Z. angew. Math. Mech. 9, 49–58.

Suquet, P., 1987. Elements of homogenization for inelastic solids. In: Sanchez-Palencia, E., Zaoui, A. (Eds.), Homogenization Techniques for Composite Media. Lecture Notes in Physics, 272, 193–278. Springer-Verlag.

Voigt, W., 1889. Über die Beziehung zwischen den beiden Elastizitätskonstanten isotroper Körper. Wied. Ann. 38, 573–587.

Zohdi, T. I., Oden, J. T., Rodin, G. J., 1996. Hierarchical modeling of heterogeneous bodies. Computer Methods in Applied Mechanics and Engineering 138, 273–298.